Assessment of Hydration Process And Mechanical Properties of Cemented Paste Backfill By Rebound Method

Sa Huang
Qingdao University of Science and Technology
Yongyan Wang (0019030005@mails.qust.edu.cn)
Qingdao University of Science and Technology
Zhuoqun Yu
Qingdao University of Science and Technology
Peng Du
Qingdao University of Science and Technology
Zhonghao Liang
Qingdao University of Science and Technology

Research Article

Keywords: uniaxial compressive strength, rebound method, functional model, overall strength, local strength

Posted Date: December 8th, 2021

DOI: https://doi.org/10.21203/rs.3.rs-951071/v1

Assessment of hydration process and mechanical properties of cemented paste backfill by rebound method

Sa Huang[1], Yongyan Wang[1,*], Zhuoqun Yu[1], Peng Du[1], Zhonghao Liang[1]

1 School of Mechanical and Electrical Engineering, Qingdao University of Science and Technology, Qingdao 266061, China

corresponding author:
Yongyan Wang (0019030005@mails.qust.edu.cn)
other authors:
Sa Huang (1075774839@qq.com), Zhuoqun Yu (yzqun2007@126.com), Peng Du (pok009@126.com), Zhonghao Liang (694213664@qq.com)

Abstract

Backfilling mining method is a green mining method which is being used widely, nevertheless, the uniaxial compressive strength (UCS) of the cement backfill paste (CPB) on site is difficult to measure, and it is impossible to know the internal cementation, for this reason, the rebound method is improved and introduced in this paper. Standard specimens of CPB were made and cured for different curing age under standard curing conditions. The hardness test of each part of the CPB is completed, the unconfined compression test is carried out, and the functional model of the hardness of each part of the CPB is established, which was a function of radius and age. Based on the nonuniformity of the filling material, the failure mode of CPB is analyzed and verified in the test. The results show that the exponential function model is more suitable for the relationship between the external hardness and the overall strength, and this conclusion is of great significance in construction site. In addition, the corresponding relationship between hardness and local strength was calculated and verified, the results show that the simple model can predict the variation of local strength with hardness better, and the quadratic function model is the best choice.

KEYWORDS: uniaxial compressive strength; rebound method; functional model; overall strength; local strength

1. Introduction

In recent decades, in order to promote the construction of ecological mines and reduce safety accidents in underground mines, the backfilling mining method has been widely used all over the world. Quite a few scholars have participated in the research of cement paste backfill (CPB) and achieved fruitful results [1-6]. Uniaxial compressive strength (UCS) is the most intuitive and important index to measure the mechanical properties of CPB. At present, most scholars study the CPB by making the standard cylindrical specimen of the backfilling body[7] in the laboratory or coring from backfill stopes at construction site [8-10], then carrying out various mechanical tests on it. Uniaxial

compression test is usually used to measure the UCS of backfilling specimens. This method only reflects the overall strength of the CPB, but the local strength and cement cementation of each part of the CPB can not be known. Under the condition of the same curing age, the hydration of cement[11] is inconsistent from the outside to the inside. Generally, the closer to the outside, the higher the degree of hydration reaction is. This is because the protective membrane[12] formed in the process of cement hydration limits the internal cement hydration reaction. Sandrine et al confirmed that calcium silicate hydrate (C-S-H) grows at the solid-solution interface and gradually forms a diffusion barrier around the anhydrous which limits the progress of the reaction[13]. Scrivener et al also introduced the Protective Membrane Theory[14]. If it is impossible to measure the cement handover inside the CPB, the failure form analysis and stress distribution analysis will be troubled. In addition, Uniaxial compression test requires not only large-scale experimental instruments, but also cumbersome steps. This condition may not be achieved in practical engineering, and coring method will inevitably cause damage to the backfill stopes. If the micro electron microscope is used for observation, the internal cementation of the CPB can be directly observed. However, due to powder to be sampled for the micro electron microscope test, after the block is transformed into powder, the specific surface area increases geometrically, the contact area with air increases greatly, the hydration reaction proceeds rapidly, and the cementation has changed. There is a large deviation from the original internal situation of the test specimens .

Up to now, studies have explored the method of indirectly measuring the strength of CPB, such as ultrasonic pulse velocity (UPV) method was used to predict the UCS of CPB prepared from three different tailings [15]. Xu et al used electrical resistivity measurement to assess of hydration process and mechanical properties of CPB [16]. Yan et al. used Fiber Bragg Grating (FBG) sensors to monitor the samples as internal strain [17].

In this paper, another nondestructive testing method is introduced to assess hydration process and mechanical properties of CPB, that was rebound method. The main idea of rebound method is to use hardness to measure strength. The batching and filling of concrete are the same, which are composed of aggregate, cement and water. The difference between the two only lies in the diverse types of aggregate. Therefore, we can learn from the methods in the field of concrete. The rebound method [18] in the field of concrete can estimate the strength through the hardness of concrete without damage quickly and concisely, and the use of rebound number method produces results that are reliable [19]. Most importantly, in the case of low strength, the correspondence between hardness and strength is better [20]. However, this method can not be applied to the backfilling body directly. There are two reasons behind this: first, the hardness range of CPB is quite different from that of concrete, and the instrument used for concrete is not suitable for CPB. Second, the concrete rebound method to detect solid strength is a method to indirectly reflect the overall strength of concrete through the surface hardness of concrete. The key point is the surface hardness of concrete. If the ratio of internal and external hydration degree between CPB and concrete is large, the prediction with the existing strength test curve will produce large errors. Therefore, this method is not

suitable for CPB because of the ratio of internal and external hydration reaction is too large at the same curing age. In view of these two reasons, we can find a suitable hardness tester and establish the strength test curve belonging to the CPB.

Based on the above background, this paper improves the rebound method and introduces it into the CPB for theoretical analysis and experimental verification.

2. Materials and methods

2.1. Materials and properties

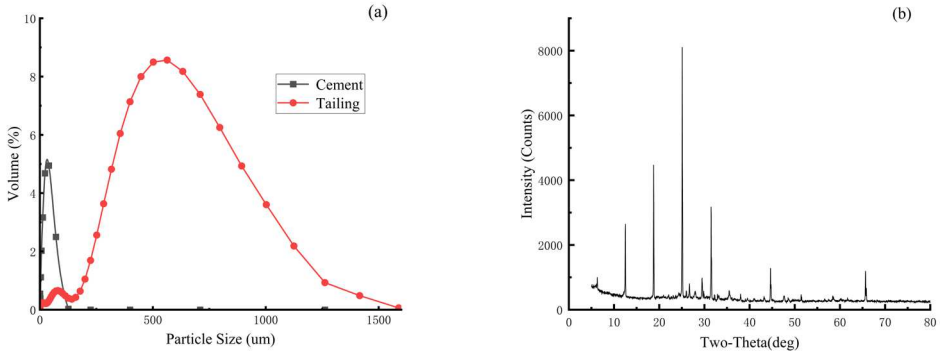

Fig. 1 (a) Particle size distribution of the tailings and cement; (b) XRD pattern of tailings.

Iron mining tailing, binder and water were used to prepare the CPB specimens. The tailing used in this study was taken from an iron mine in Laiwu city, Shandong Province, China. The particle size distribution of the tailing was determined to use a laser particle size analyzer (Mastersizer 2000, Malvern). The particle size distribution of the tailings is presented in Fig. 1(a) and the x-ray diffraction (XRD) with Cu Ka radiation at room temperature was used to identify the crystallin components in tailings is presented in Fig. 1(b). The specific gravity of the tailings was measured to be 2.45.

The main chemical compositions of tailing are shown in Table 1. It can be seen that the main chemical compositions of tailing are Fe_2O_3, SiO_2, CaO, MgO, and Al_2O_3, accounting for 95.237% of the total tailing by weight, and the main chemical elements of tailing are Fe, Ca, Si, Mg, Al, Cu, and K, they account for 96.715% of the total tailing by weight, moreover, each of them is greater than 1 percent.

Tap water that added to mix the tailing and binder. The amount of water added to obtain the preparation of backfill mixture with solid content was approximately 75% by weight.

Reference cement (P.I42.5) was used in the test. The particle size distribution of the cement is presented in Fig. 1(a). Cement in cement-to-tailing ratio of 1/8 by weight was the binding agent.

Table 1 Main chemical properties of tailings used in this study.

Composition	Content (%)	Element	Content (%)
MgO	12.93	Mg	10.786
Al_2O_3	8.894	Al	6.754
SiO_2	27.409	Si	18.893
CaO	18.684	K	1.13
Fe_2O_3	27.32	Ca	22.088
CuO	1.067	Fe	35.364
		Cu	1.7

2.2. Specimens preparation

In this study, 8 CPB specimens were prepared in total, the specimens are prepared in terms of c/t ratio (cement-to-tailing ratio) with 1:8. The tailings and cement are weighed according to the proportion in the dry state, and mixed with water to make the solid mass concentration reach 75%.The tailing, binder and water were mixed and thoroughly homogenized about 12 min to produce the desired CPB mixtures. After mixing, the prepared CPB mixtures were poured into cylindrical moulds that were 5 cm in diameter and 10 cm in height. Demoulding after 24 hours and curing in environment chamber with controlled temperature at 20 °C and 90 ± 5% relative humidity in different curing ages, and the specimen number and curing age are shown in Table 2.

Table 2 Specimen number and curing age.

Curing age	3 days		7 days		14 days		28 days	
Specimen number	W1	W2	W3	W4	W5	W6	W7	W8

2.3. Test process

2.3.1 Uniaxial compression test

Taw-200 electronic multifunctional material mechanics testing machine (Fig. 2) was used to conduct uniaxial compression test on specimens numbered W1, W3, W5 and W7. The constant displacement loading mode with a rate of 0.2mm/min is adopted without preloading. When the indenter is about to contact the test piece, the data is recorded. After the test, the failure form of the specimens is recorded by taking photos. The stress-strain curve is shown in Fig. 3, and the results are summarized in table 3.

Fig. 2 TAW-200 electronic multifunctional material mechanics testing machine.

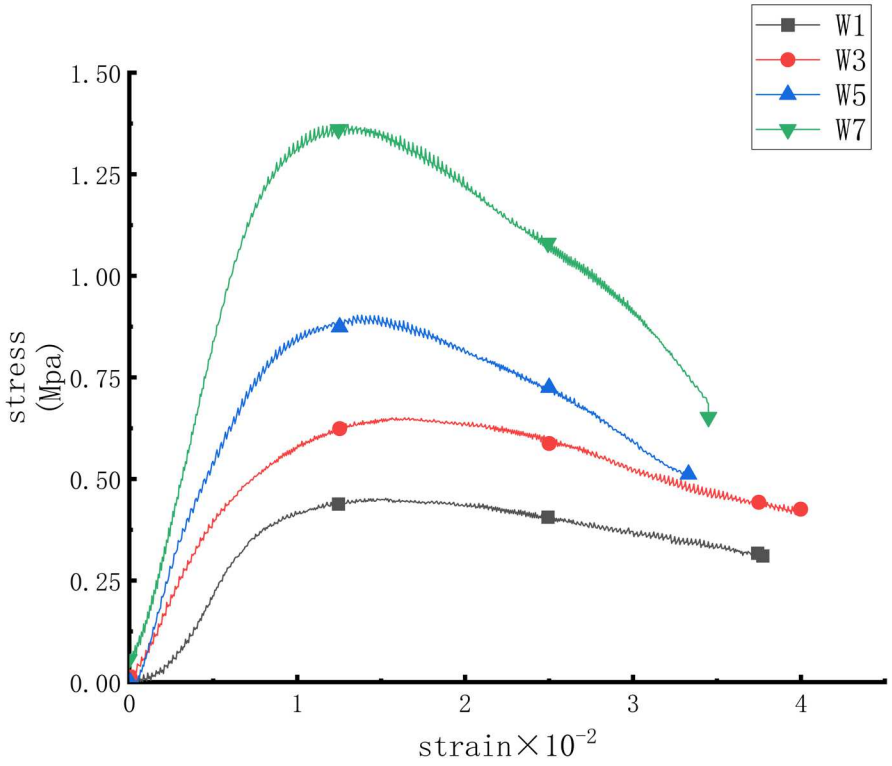

Fig. 3 stress-strain curve

Table 3 Uniaxial compression test results.

Specimen number	W1	W3	W5	W7
Uniaxial compressive strength (Mpa)	0.47	0.66	0.94	1.38

2.3.2. Hardness value test

In this paper, shore hardness tester (Lx-D type) is used to measure the hardness of backfilling body. The equipment is shown in Fig. 4. There are three specific reasons for using the equipment: first, the shore hardness tester is a needle type, which can accurately measure the hardness of a certain part; second, the measuring range of D-type shore hardness tester is consistent with the hardness range of CPB; third, the filling materials, cement and tailings, are relatively uniform fine particles, without stones and other impurities that lead to local hardness, and the hardness result error obtained by the needle hardness tester is small.

The proportion of backfilling materials used in the same filling and mining construction site is fixed, and the construction situation is often similar. If different strength test curves are designed for different sites, the problem that the existing strength test curve is not suitable for a specific construction site can be solved.

In order to avoid the influence on the internal hardness of the test piece to the greatest extent, the test pieces numbered W2, W4, W6 and W8 are split from the middle plane along the vertical cylindrical axis, and the section is smoothed. Draw circles with radius (r) of (0, 5, 10, 15, 20, 25) mm from the center of the section circle, as shown in Fig. 5. Take 5 points at the position with equal spacing on each circle, measure the hardness value respectively, remove the maximum and minimum values, take the average value of the remaining three values, and record the experimental results, as shown in Table 4.

Fig. 4 Shore hardness tester (type D).

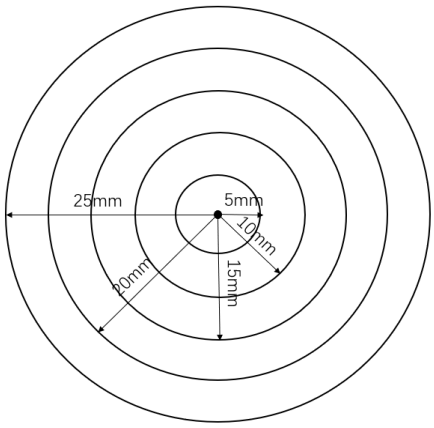

Fig. 5 Schematic diagram of hardness test.

Table 4 Test results of hardness test.

Specimen number	W2						W4					
Radius(cm)	0	0.5	1.0	1.5	2.0	2.5	0	0.5	1.0	1.5	2.0	2.5
Hardness (HD)	10	12	14	15	17	20	18	20	22	24	25	27
Specimen number	W6						W8					
Radius(cm)	0	0.5	1.0	1.5	2.0	2.5	0	0.5	1.0	1.5	2.0	2.5
Hardness (HD)	23	24	25	27	29	30	34	35	36	37	39	40

2.4 Results and discussions

The failure form of each specimen is shown in Fig. 6. We can find that the CPB specimens of each age are in the combined failure form of upper conjugate shear and middle tensile failure by observing the failure form of the specimens. Further, we find that the interior of the specimen is conical after stripping the outer layer. Take W1 as an example (Fig. 7).

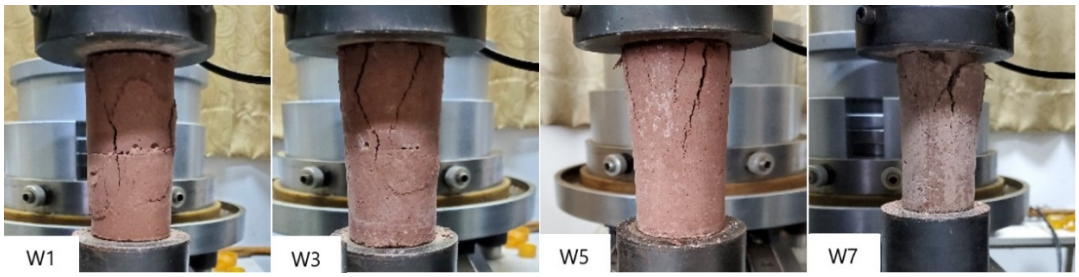

Fig. 6 Failure mode of specimens.

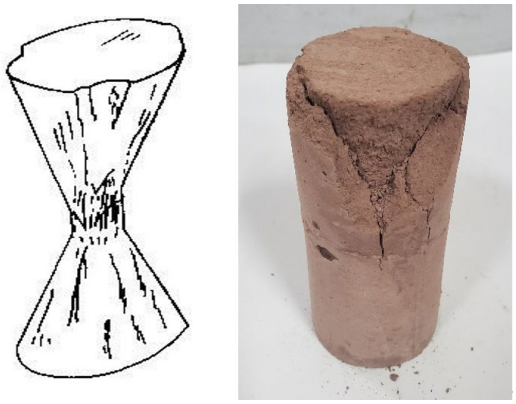

Fig. 7 Internal failure mode of specimen.

The reasons for its formation are analyzed: under the action of compressive stress, the specimen shortens in the axial direction and expands in the transverse direction. The friction between the end of the specimen and the indenter restricts its transverse deformation. According to the Saint Venant's Principle, the farther away from the force point, the more uniform the stress is. Therefore, conjugate shear failure is formed at the end and tensile failure is formed in the middle far away from the end, a conical failure form is formed inside. Coulomb's Maximum Principal Shear Stress Theory can explain the formation mechanism of conjugate fracture. According to his theory, the shear angle is obtained by the Eq. (1):

$$\Phi = 45^o - \frac{\rho}{2} \qquad (1)$$

Where Φ is the conjugate shear angle, ρ is the internal friction angle. The premise of this conclusion is that the specimen material is uniform and the mechanical properties of each part are consistent.

Under certain circumstances, the hardness value reflects the cementation of each part of the CPB specimen. By analyzing the hardness value test results in Table 4, it is

not difficult to find that the cementation of each part of the backfilling body test specimen is not consistent, but gradually increases from the inside to the outside. The internal friction angle is closely related to the cementation of the CPB specimens. The better the cementation of the test specimens, the greater the internal friction angle is. Therefore, from the outside to the inside, the shear angle gradually increases, which explains why the shear angle of the same specimens is not fixed in the test.

From the experimental results of hardness values in Table 2, we can clearly find that the hardness values of CPB specimens at various ages gradually increase from the inside to the outside, showing a roughly linear distribution. This is because the hydration reaction is carried out step by step from the outside to the inside. The external hydration reaction will form a "Protective membrane" to prevent the internal hydration reaction from continuing.

In addition, the strength changes of each specimen at the center of the circle and the outer surface are compared. Among them, the strength ratio of part W2 at the center of the circle to the outer surface is 50%, W4 is 66.7%, W6 is 76.7%, and W8 is 85%. This shows that there are obvious differences between the surface and internal quality of the specimens, especially the specimen at middle and low ages. However, with the increase of age, the mechanical properties of each part of the specimen tend to be consistent. To sum up, in the numerical calculation of the CPB specimen, it can not be regarded as homogeneous material, and the influence of different cementation of each part must be considered.

3 Model establishment and verification

3.1 Functional model of each part of the specimens

The hardness values of the four test specimens in the table are calculated by Eq. (2).

$$h = ar + b \qquad (2)$$

Linear fitting is carried out respectively, where h is the hardness value, a and b are parameters, and r is the distance to the center of the circle. The fitting results are summarized in Table 5. We find that the goodness of fit of each fitting equation is very high from Table 5, each of them is greater than 0.96, which ensures the reliability of the fitting equation models.

Table 5 Fitting equation of hardness at each part of test piece.

Specimen number	W2	W4	W6	W8
Parameter a	3.8	3.4	3.2	2.6
Parameter b	9.9	18.5	22.2	33.5
Fitting Eq	h=3.8r+9.9	h=3.4r+18.5	h=3.2r+22.2	h=2.6r+33.5
Goodness of fit (R^2)	0.96057	0.9863	0.97949	0.97674

Fitting the parameters a and b with the curing age t respectively, we find that there is a functional relationship among the parameters a, b and the curing age t, the results

are shown as Eq. (3) and Eq. (4):

$$a = 3.88883 \times 0.98559^{t} \quad (3)$$

Goodness of fit R^2=0.97401

$$b = 56.72803 \times e^{-\frac{20.06268}{t+9.14273}} \quad (4)$$

Goodness of fit R^2=0.97086

Replace Eq. (3) and (4) into formula 2 to obtain the functional model of hardness of each part of the specimen, as shown as Eq. (5).

$$h = 3.88883 \times 0.98559^{t} \times r + 56.72803 \times e^{\frac{-20.06268}{t+9.14273}} \quad (5)$$

3.2 Functional model between external hardness and overall strength

The most intuitive and easily obtained hardness data is the external surface hardness of the backfilling body (r=25mm). If the functional relationship between the external surface hardness and the overall strength can be established, it will bring great convenience to estimate the overall UCS of the backfilling body in engineering application. To look for a suitable fitting function, we fit it with linear function model, quadratic function model and exponential function model respectively. The results are shown in Fig. 8.

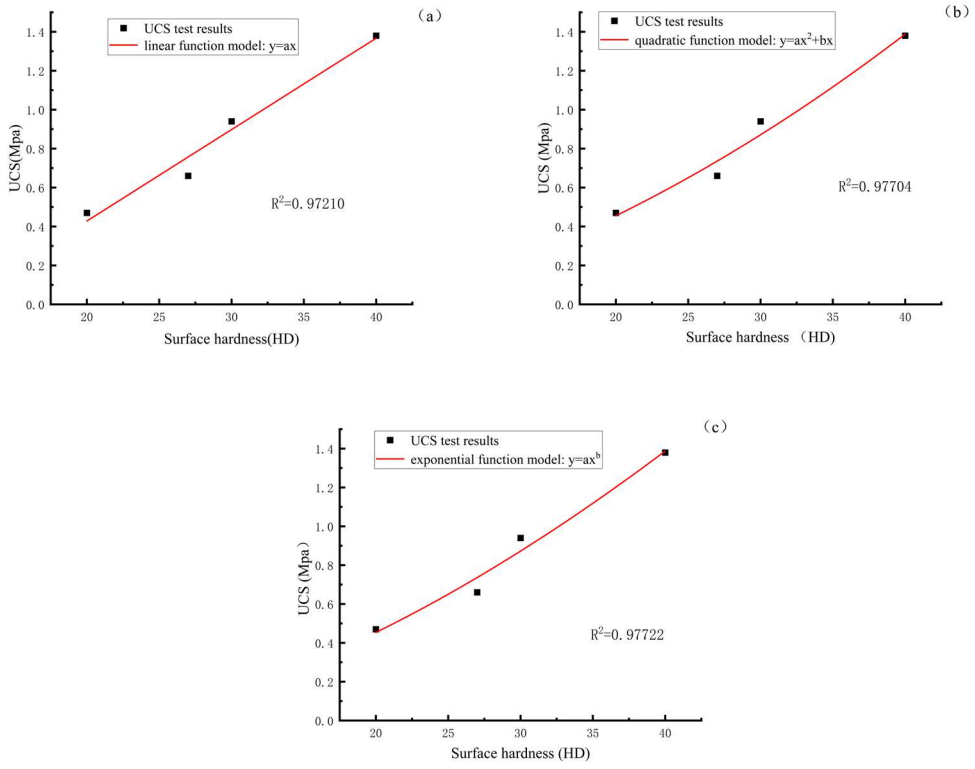

Fig. 8 Functional model, (a) linear function model; (b) quadratic function model; (c) exponential function model.

The results show that the three functions can fit them well, which proves that there

is a reliable functional correspondence between the external hardness and the overall strength of the CPB, and the exponential function is the optimal choice.

3.3 Functional model between hardness and local strength

Compared to overall strength, local strength is also of great significance in the field of CPB. the corresponding function of hardness value and local strength need to be established. Rebound method in concrete field, the corresponding function (strength test curve) of concrete rebound value and UCS at different strength stages is also different. Considering the low strength of the CPB, the corresponding function curve [21] of young concrete with low compressive strength is used as the quadratic function model, which was shown as Eq. (6).

$$f = \mathrm{cD}^2 + \mathrm{dD} \qquad (6)$$

Where f is the local strength, c and d are parameters, and D is the rebound value. Since the rebound value is directly proportional to the hardness, Eq. (7) can be obtained.

$$f = \mathrm{c_1h}^2 + \mathrm{d_1h} \qquad (7)$$

Where c_1 and d_1 are parameters. The overall strength is the local strength of each part multiplied by $2\pi r$ is divided by the cross-sectional area of the specimens after integrating along radius [22].

$$F_c = \frac{\int_0^{0.025} 2\pi r \times f dr}{\pi R^2} \qquad (8)$$

Where F_C is the overall strength, R is the radius of the specimens. By substituting the data of any two data, we can get the expression of the eq. (8). Taking the W1 and W7 as an example, the calculation results can be obtained, $c_1 = 130.643$, $d_1 = 36758.645$.

Substitute c_1 and d_1 into Eq. (8) and we can get the Eq. (9).

$$F_c = 0.62 \times 0.98559^{2t} + 960.66 \times 0.98559^t \times e^{\frac{-20.06268}{t+9.14273}} + 420408.59 \times e^{\frac{-40.12536}{t+9.14273}} + 2382.47 \times 0.98559^t + 2085245.23 \times e^{\frac{-20.06268}{t+9.14273}} \qquad (9)$$

Kovler et al. confirmed that linear regression was more reliable for rebound curve [23]. so it is assumed that the hardness value is a linear function of uniaxial compressive strength as Eq. (10):

$$f = ih \qquad (10)$$

Where i is a parameter. The value of parameter i can be obtained by substituting the data of any age. Taking the data of W5 as an example, the calculation result is i=3.92×10^4. The expression of the overall strength is shown as Eq. (11):

$$F_c = 2537.46 \times 0.98559^t + 2220903 \times e^{\frac{-20.06268}{t+9.14273}} \qquad (11)$$

Since then, we have obtained two different expressions of strength with respect to curing age t from the perspective of local strength of CPB.

3.4 Results verification

For a clearer comparison, the whole age fitting verification of Eq. (9) and Eq. (11)

is carried out. The results are shown in Table 6. It can be found that the calculated results of the two functional models are consistent with the measured results. It proves that the simple function can well reflect the relationship between hardness and strength, which is consistent with the research results of some scholars [24,25]. Among the two functional models, the quadratic model has better prediction effect in the old age, and the primary function model has better prediction effect in the young age. The R^2 of the quadratic model is slightly higher than that of the primary model. The quadratic model is generally better, and the quadratic term coefficient c_1 of Eq. (7) is larger, which means that the curvature of the quadratic function curve is small and approximately linear. It can be understood that the relationship between local strength and hardness is approximately linear, which is the reason why the primary function model can also better reflect the relationship between local strength and hardness.

Table.6 Results verification.

Curing age t (days)	3	7	14	28	R^2
Measured results	0.47	0.66	0.94	1.38	--
Eq. (9)	0.42	0.64	0.95	1.36	0.9972
Eq.(11)	0.43	0.64	0.94	1.30	0.9942

4 Discussion

Each function model obtained and verified in this section has different functions in practical engineering application. The function model of the hardness of each part of the specimen with respect to radius *r* and age *t* can help the front-line construction personnel to understand the cementation in the backfilling body. The function model between external hardness and overall strength can easily, concisely and quickly obtain the UCS of the CPB, which reduces the workload of first-line construction. The functional model between hardness value and local strength can help scholars understand the mechanical properties of each part of the CPB, which is very helpful to the research work. The function model obtained and verified in this section can not be applied to different mining sites, but the method of establishing the model is universal. The working conditions in the same construction mine are often the same, such as ash sand ratio, mine master size, etc. Therefore, the specific function model can be established according to the method in this paper according to the specific conditions. The limitation is that the research contents and conclusions of this paper are only applicable to upward horizontal slice filling method and other backfilling methods with filling pillar.

5 Conclusions

1. In this paper, the rebound method is introduced and improved to measure the hardness of each part of the CPB specimen. The results show that the cementation of each part of the specimen is different at different ages, and the expression of hardness change from inside to outside is fitted.

2. Combined with the experimental results, the failure form of the specimens is analyzed, and the reason why the conjugate shear angle of the specimens increases from outside to inside is explained.

3. The relationship between the external hardness and overall strength of the backfilling specimens is explored, and it was found that the exponential function is more suitable for the specimens in this test. Although different backfilling mining site may be suitable for different function models, the appropriate function model can be established according to the method in this paper. According to this, this method can be extended to engineering application for nondestructive testing.

4. The corresponding relationship between hardness and local strength of each part of the specimen is calculated and verified. The results show that the simple function model can well predict the change of local strength with hardness, and the quadratic function model is the optimal choice.

5. From the perspective of uneven materials, this paper studies the variation law of internal and external hardness of the CPB, breaking the conventional view that the CPB is regarded as a whole material, which is of great significance to the follow-up research.

References

1 Chen, S. *et al.* Effects of chloride on the early mechanical properties and microstructure of gangue-cemented paste backfill. *Construction and Building Materials* **235**, 117504 (2020).

2 Cihangir, F. & Akyol, Y. Mechanical, hydrological and microstructural assessment of the durability of cemented paste backfill containing alkali-activated slag. *International Journal of Mining, Reclamation and Environment* **32**, 123 - 143 (2018).

3 Fall, M. & Pokharel, M. Coupled effects of sulphate and temperature on the strength development of cemented tailings backfills: Portland cement-paste backfill. *Cement & Concrete Composites* **32**, 819-828 (2010).

4 Qi, C. *et al.* Towards Intelligent Mining for Backfill: A genetic programming-based method for strength forecasting of cemented paste backfill. *Minerals Engineering* **133**, 69-79 (2019).

5 Wu, D., Fall, M. & Cai, S. Coupling temperature, cement hydration and rheological behaviour of fresh cemented paste backfill. *Minerals Engineering* **42**, 76-87 (2013).

6 Xie, S. *et al.* Experimental and mechanistic research on modifying the mechanic properties of the high water backfill material by electrochemical treatment. *Scientific Reports* **10** (2020).

7 Vol. GB/T 39489-2020.

8 Deng, D., Jiang, N. & Duan, Y. Sampling and Mechanical Testing of Backfill in Large Mined-Out Area. *Geofluids* **2021**, 1-8 (2021).

9 Vance, G., Fadlemawia, A. A., See, R. B. & Reddy, K. Role of Natural Organic Solutes on the Sorption of Selenium by Coal Mine Backfill-Core Samples from the Powder Basin, Wyoming. *Journal of the American Society of Mining and Reclamation* **1995**, 246-257 (1995).

10 Zhang, X. & Zhang, S. Experimental Investigation on Mechanical Properties of In Situ

Cemented Paste Backfill Containing Coal Gangue and Fly Ash. *Advances in Civil Engineering* **2020**, 1-12 (2020).

11 Chatterji, A. & Phatak, T. C. Hydration of Portland Cement. *Nature* **207**, 711-713 (1965).

12 Bullard, J. *et al.* Mechanisms of cement hydration. *Cement and Concrete Research* **41**, 1208-1223 (2011).

13 and, S. G. & Nonat, A. Hydrated Layer Formation on Tricalcium and Dicalcium Silicate Surfaces: Experimental Study and Numerical Simulations. *Langmuir* **17**, 8131-8138 (2001).

14 Scrivener, K., Ouzia, A., Juilland, P. & Mohamed, A. K. Advances in understanding cement hydration mechanisms. *Cement and Concrete Research* (2019).

15 Z1lmaz, T. & Erçikdi, B. Predicting the uniaxial compressive strength of cemented paste backfill from ultrasonic pulse velocity test. *Nondestructive Testing and Evaluation* **31**, 247 - 266 (2016).

16 Xu, W., Tian, X. & Cao, P. Assessment of hydration process and mechanical properties of cemented paste backfill by electrical resistivity measurement. *Nondestructive Testing and Evaluation* **33**, 198 - 212 (2018).

17 Yan, B., Zhu, W., Hou, C., Yu, Y. & Guan, K. Effects of coupled sulphate and temperature on internal strain and strength evolution of cemented paste backfill at early age. *Construction and Building Materials* **230**, 116937 (2020).

18 Vol. JGJ/T 23-2011 68P.

19 Shang, H., Yi, T. & Yang, L. Experimental Study on the Compressive Strength of Big Mobility Concrete with Nondestructive Testing Method. *Advances in Materials Science and Engineering* **2012**, 1-6 (2012).

20 Szilágyi, K., Borosnyói, A. & Zsigovics, I. Understanding the rebound surface hardness of concrete. *Journal of Civil Engineering and Management* **21**, 185-192 (2015).

21 *SilverSchmidt. Available online: https://www.proceq.com/uploads/tx_proceqproductcms/import_data/files/SilverSchmidt_Operating%20Instructions_English_high.pdf (accessed on 21 June 2019).*

22 Wang, Y.-Y., Fan, X., Qin, N., Li, J.-G. & Su, C. The Theory and Demonstration of the Solid-Fluid Transformation of Ice Water. *Advances in Mathematical Physics* **2020**, 1-8 (2020).

23 Kovler, K., Wang, F. & Muravin, B. Testing of concrete by rebound method: Leeb versus Schmidt hammers. *Materials and Structures* **51**, 1-14 (2018).

24 Kim, J.-k., Kim, C.-Y., Yi, S. & Lee, Y. Effect of carbonation on the rebound number and compressive strength of concrete. *Cement & Concrete Composites* **31**, 139-144 (2009).

25 Kocáb, D., Misák, P. & Cikrle, P. Characteristic Curve and Its Use in Determining the Compressive Strength of Concrete by the Rebound Hammer Test. *Materials* **12** (2019).